New Strategies for Probing Crystal Dissolution Kinetics at the Microscopic Level

Patrick R. Unwin and Julie V. Macpherson
Department of Chemistry, University of Warwick, Coventry CV4 7AL, U.K.

1 The Nature of Dissolution Reactions

The process of dissolution of a solid in a liquid is generally considered to be one of the simplest chemical reactions, and is often written in terms of a simple equation, for example, for an ionic crystal dissolving in an aqueous solution:

$$M_yX_{z(s)} \rightleftharpoons yM^{z+}_{(aq)} + zX^{y-}_{(aq)} \quad (1)$$

Equation 1 defines the net result of dissolution, *i.e.* the transfer of ions from a solid, M_yX_z, to an undersaturated solution, but masks the complexity of dissolution mechanisms.

When a solid dissolves in a liquid, the overall reaction may be represented in terms of some or all of the series of elementary events, illustrated schematically in Figure 1: (i) detachment of ions or molecules from a dissolution site; (ii) surface diffusion of the detached species; (iii) desorption (and adsorption); (iv) mass transfer away from the crystal. The latter step is usually the movement of material into the bulk of solution (by diffusion, convection, and perhaps migration) but may also include diffusion through a porous layer at the solid surface. Steps (i) to (iii) are surface processes and when any of these steps is slow compared to the transport processes, the dissolution reaction is said to be kinetically *surface controlled.* Conversely, when the surface processes are fast compared to the transport processes [step (iv)], the reaction is termed *transport controlled.*

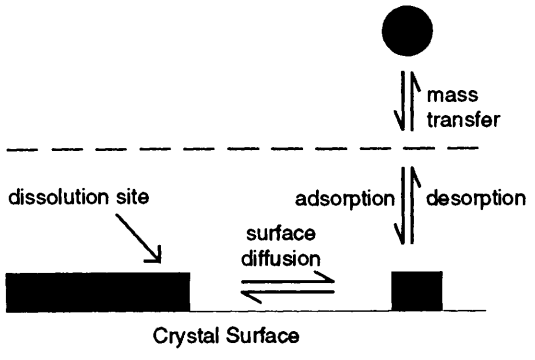

Figure 1 Schematic of the elementary steps involved in dissolution processes.

The picture of dissolution given in Figure 1 is further complicated when one considers the nature of a typical crystal in more detail. For many crystalline materials, the morphology is such that a variety of crystal faces are exposed. As is generally recognized in surface science,[1] faces of a crystalline material with different arrangements of atoms, ions, or molecules (depending on the nature of the material) are often characterized by different reactivities. Furthermore, as illustrated schematically in Figure 2, even on a single crystal face there is a considerable variety of defects and surface microstructure, such as steps, terraces, kink sites, vacancies, and adatoms, along with screw and edge dislocations, all of which have characteristic free energies of dissolution. Thus at an elementary level, a number of dissolution mechanisms (and rates) may operate in parallel over a single crystal surface.

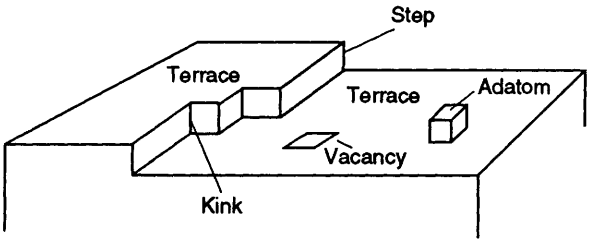

Figure 2 Schematic of some of the important elementary features on a typical single crystal surface.

It follows from this brief introduction, that in order to understand the mechanisms and kinetics of dissolution processes, experimental studies should be able to provide answers to the following key questions:

(i) *What is the relationship between surface structure and reactivity*? This includes the ability to study the reactivity of both an individual crystal surface and a particular structural feature on a surface.

Patrick Unwin was born in Great Preston, West Yorkshire in 1964 and educated at the University of Liverpool and the University of Oxford. Following periods as Junior Research Fellow in Physical Sciences at Balliol College (1988—91) and as a NATO Fellow at the University of Texas at Austin (1990—91), Dr. Unwin was appointed to a Lectureship in Physical Chemistry at the University of Warwick in 1991. Research interests lie in the areas of dynamic electrochemistry and interfacial chemistry.

Julie Macpherson was born in Sutton Coldfield in 1972. She obtained a First class Honours degree in Chemistry from the University of Warwick in 1993 and was awarded the RSC Electrochemistry Group undergraduate project prize for her initial work in the area of scanning electrochemical microscopy (SECM). Julie Macpherson is currently working towards a Ph.D. on the development and application of SECM, particularly for studying dissolution processes.

(ii) *What role does local mass transfer play in controlling the dissolution rate*? For a particular face (or preferably a specific feature on a crystal face), is the rate controlled by mass transport in solution, a surface process, or under mixed kinetic control? If there are surface kinetic limitations, which surface process limits the rate? It also follows that if fast surface processes are to be characterized, techniques must be able to deliver mass transport rates which are sufficiently high to compete with the kinetics of the surface reactions.

(iii) *How does the rate and mechanism depend on local undersaturation at the solid/liquid interface*? This question recognizes that the level of undersaturation at the crystal/solution interface provides the driving force for dissolution and not that in the bulk of solution.

Although there have been a very large number of studies of dissolution kinetics,[2] driven by the importance of dissolution processes in a number of areas of chemistry and its borders with physics,[3] environmental science,[4] and biology,[5] it is only comparatively recently that experimental techniques have become available which are able to address quantitatively some or all of the above questions. The general aim of this review is to assess critically some of the important developments in the field of dissolution kinetics and to identify the current level of understanding of this significant class of reactions. Particular emphasis will be given to the dissolution of ionic crystals in aqueous solutions, which are among the most important reactions of this type.

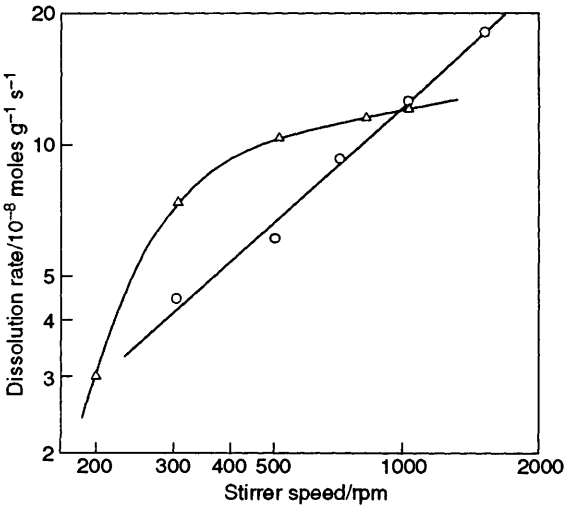

Figure 3 Rate–stirring speed characteristics for the dissolution of calcite fragments (125—250 microns in size) in 0.7 mol dm^{-3} KCl at pH 8.4 and 25 °C. The different symbols relate to experiments performed in a round-bottomed vessel without baffles (△) and in a rotating disc vessel with baffles (○). The plateau in the rate in the former case corresponds to the particles becoming fully suspended.
(Redrawn with permission from E. L. Sjöberg and D. Rickard, *Geochim. Cosmochim. Acta*, 1983, **47**, 2281.)

2 Conventional Methods: The Need for New Approaches

The majority of dissolution studies have employed solid particles stirred in a liquid, with kinetic and mechanistic information inferred from changes in the chemical composition of the bulk solution, measured as a function of time.[2] While this general approach has allowed average rates to be measured, there are several inherent drawbacks in the mechanistic interpretation of rate data thus obtained. First, the use of particles, which comprise various exposed faces (and amorphous material), makes it difficult to investigate the effect of surface structure on the dissolution rate and mechanism. Secondly, mass transfer in particulate systems depends on a large number of parameters, such as the geometry of the reaction vessel, type of baffles and stirrer, speed of stirrer, slurry density, liquid density and viscosity, diffusion coefficients of reactants and products, along with the geometry, density, and size distribution of the particles.[6] Consequently, 'there is no reliable general correlation of mass transfer coefficients for such systems' (reference 6) and investigating the extent to which mass transfer controls even the average dissolution rates of particles has proved to be difficult.

The importance of mass transport in the rate of heterogeneous reactions has often been determined by investigating the effect of stirring rate on the reaction rate. A lack of stirring dependence is taken to imply a lack of transport control in the reaction, *i.e.*, that the rate is controlled by a surface process. However, for particulate systems, with poorly defined hydrodynamics, it has been demonstrated that a lack of stirring dependence of the reaction rate may simply mean that the hydrodynamic environment around a particle does not change with stirring speed,[7] as opposed to the dissolution process becoming surface controlled. Figure 3 illustrates this point, showing rate data for the dissolution of calcite particles as a function of stirrer speed measured under two sets of conditions: in a standard rotating disc vessel with baffles (○); and in a round-bottomed reaction vessel without baffles (△). The data in Figure 3 demonstrate that the dissolution rate–stirring speed characteristics can vary dramatically simply by changing the shape of the reaction vessel. The implications are that, for experiments with particulates, the extrapolation of results from one laboratory study to another may be difficult.[7]

A further disadvantage of particulate-based experiments is that the measurement of chemical changes in bulk solution, distant from the reaction site, can 'only provide indirect information about processes occurring at or near the solid/liquid interface' (reference 7). Under these conditions, the level of undersaturation in the bulk of solution is considered to be the driving force for dissolution, rather than that at the solid/liquid interface, which is clearly inappropriate. Moreover, for certain types of investigations, the implicit batch nature of particulate systems dictates that measurements are restricted to short times in order to avoid significant changes in the solution composition during the course of a measurement.[2]

3 Techniques with Well-defined Hydrodynamics

In order to overcome the problem of ill-defined mass transfer, techniques possessing well-defined hydrodynamics have been adopted. Such techniques allow mass transport to be varied in a controlled and calculable manner over a wide dynamic range. In this section we assess the advantages and disadvantages of the rotating disc method[7—12] and of the channel flow method with electrochemical detection,[13—18] which are among the most popular techniques of this type.

3.1 Rotating Disc Method (RDM)

This approach can be considered to be derived from the rotating disc electrode, which has found considerable application in the study of electrode reactions.[19] For the investigation of dissolution processes, the solid of interest is cast flush in the end of a cylinder of inert material (*e.g.*, epoxy resin) so that a disc of the solid is exposed in the centre of the cylinder end. The cylinder is attached to a motor which is used to rotate the solid disc about its centre in a solution. The rate of mass transport of solution species to and from the disc can be controlled by varying the rotation speed, and the well-defined hydrodynamics (for practical devices operated under laminar flow conditions) permit the calculation of the corresponding mass transport rates.[20]

The RDM has found widespread application as a powerful approach for investigating the importance of mass transport *versus* surface control on the average rate of dissolution of a solid material.[7—12] To illustrate the type of information which can be obtained with the RDM, Figure 4 shows results for the dissolution of calcite in aqueous solution at pH 8.4. In contrast

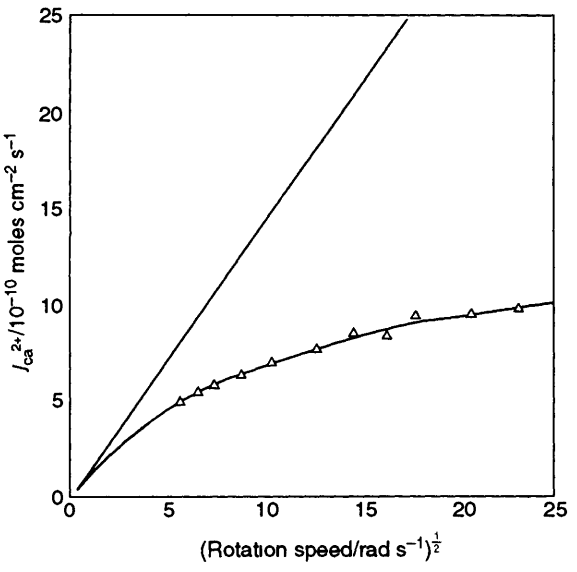

Figure 4 Rate rotation speed characteristics for the dissolution of calcite in aqueous 0 7 mol dm ^{3} KCl at pH 8 4 and 25 °C (△) The straight line represents the behaviour predicted for a purely diffusion-controlled reaction [20]
(Redrawn with permission from D T Rickard and E L Sjoberg, *Am J Sci*, 1983, **283**, 815)

to the behaviour in Figure 3, the dissolution rate (defined in terms of the interfacial flux of calcium, $J_{Ca^{2+}}$) – rotation speed curve can be described quantitatively in terms of a transport constant, k_T, and a dissolution rate constant, k_c [10]

$$J_{Ca} = \frac{k_c k_T (c_{eq} - c_b)}{k_c + k_T} \quad (2)$$

where c_{eq} and c_b are the calcium carbonate concentrations, defined as the mean concentration of free Ca^{2+} and CO_3^{2-} ions, in a saturated solution and in the bulk solution, respectively The well-defined hydrodynamics of the rotating disc allows k_T to be written precisely in terms of the rotation frequency, ω (Hz), the kinematic viscosity of the solution, ν, and the diffusion coefficient of the dissolving species, D

$$k_T = 1\ 554 D^{2/3} \nu^{-1/6} \omega^{1/2} \quad (3)$$

The average dissolution rate constant can thus be accurately determined, in this case[10] as 6×10^{-3} cm s $^{-1}$

An additional merit of the RDM is that when the material of interest is available in the form of a single crystal, kinetic measurements may be carried out on a (reproducibly prepared) individual face [7 10 12] Moreover, if microscopy studies of the exposed face of interest are carried out post-reaction, it is possible to correlate average kinetic measurements with microscopic structural changes resulting from dissolution An elegant example of this approach is in the study of the dissolution of the (111) face of potassium aluminium sulfate,[12] where a series of rate measurements were made as a function of undersaturation, with the corresponding dissolution etch-pit patterns at each undersaturation measured microscopically, *ex situ* This study demonstrated that there was a characteristic threshold interfacial undersaturation for the formation of an etch-pit at a dislocation site The value of the undersaturation necessary for etch-pit nucleation was shown to depend on the nature of the dislocation, with dislocations characterized by the ⟨100⟩ Burgers vector requiring a higher interfacial undersaturation than those with the ⟨110⟩ Burgers vector

The RDM represents a significant improvement on particulate based methods, in that it allows questions (i) to (iii), outlined in Section 1 to be addressed at the level of a single crystal face Moreover, there is the possibility of correlating average rate data with changes in the microtopography of the surface Disadvantages derive from the batch nature of the technique As with particulate based systems, interfacial fluxes are not probed directly, but are inferred from temporal changes in the chemical composition of the bulk solution, while the accumulation of dissolution products in the reaction medium often restricts measurements with the RDM to short times

3.2 Channel Flow Method with Electrochemical Detection (CFMED)

In this approach, the solid of interest, typically in crystalline form, is located in one wall of a channel (rectangular duct), as shown schematically in Figure 5, through which a solution is flowed under laminar conditions A detector electrode (amperometric[13–16] or potentiometric[17 18]) is located immediately downstream of, and adjacent to, the crystal surface This is used to measure the concentration of reactant(s) or dissolution products reaching the electrode surface, which, in turn, is governed by the kinetics of the dissolution reaction [13 18] The geometry of the channel is such that $2h \ll d$ and $w < d$ (see Figure 5 for definitions of the terms) so that the crystal and electrode effectively see a two-dimensional parabolic flow profile [21] In typical experimental practice, h is in the range 0 1—0 5 mm, d is in the range 6—12 mm, and $w \approx 0\ 8\ d$ For maximum sensitivity to the interfacial process, the detector electrode is made as short as possible compared with the crystal length,[22] which is typically of the order of 2—5 mm

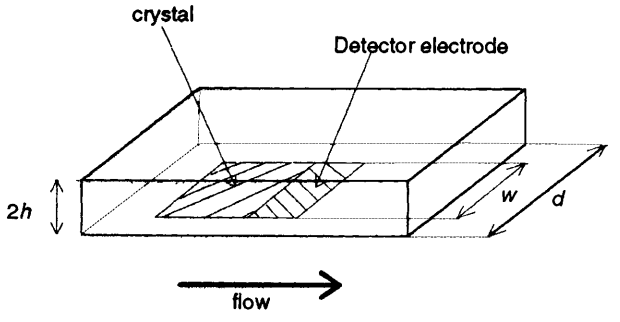

Figure 5 Schematic of the channel flow geometry for dissolution studies using the CFMED

The CFMED retains the attractive features of the RDM in that studies may be carried out on a single crystal face[13 18] under conditions where the transport of species to and from the reactive interface (and the detector electrode) is well defined, calculable, and controllable [21] Additional advantages result from the geometry shown in Figure 5 First, precise chemostatic control of the reaction environment may be exercised reactants flow into the channel at the upstream end and products flow to waste downstream, rather than accumulate in the reaction medium Secondly, the detector electrode measures either the local flux (in the case of an amperometric electrode)[13 16] or local concentration (in the case of a potentiometric electrode)[17 18] of a target solution species, which can be described in terms of the corresponding flux (and concentration) distribution at the crystal/solution interface [13 18] The dissolution rate law can thus be deduced in terms of the interfacial undersaturation Additionally, transient phenomena can readily be identified, since changes in the interfacial rate are reflected in the time-dependence of the detector electrode response

The CFMED has found considerable application in studies of the dissolution kinetics and mechanisms of natural carbonate minerals in aqueous solutions, such as calcite[13 17] and dolomite,[15] along with related limestones and chalks [16] The effect of several potential inhibitors, including a range of carboxylate anions[14] and divalent metal ions,[18] has also received attention

One of the attractive features of the CFMED is the possibility of characterizing a wide range of heterogeneous reactivities, since mass transport rates can be delivered over a wide range, by simultaneously varying the geometries of the channel, crystal, and electrode, together with the volume flow rate employed [21] The availability of high mass transport rates (by operating with thin channels, short crystals and electrodes, and fast volume flow rates) has proved to be particularly useful in characterizing fast surface processes This approach, for example, led to the first determination of the interfacial rate law for calcite dissolution at low pH (3—4),[13] a process which a large number of previous studies had found to be transport controlled The reaction was studied by flowing an HCl solution of the desired pH over a calcite crystal with the (100) face exposed, and monitoring the flux of protons at a platinum electrode located downstream, through transport-controlled reduction to hydrogen The heterogeneous reaction at the crystal surface

$$H^+_{(aq)} + CaCO_{3(s)} \xrightarrow{k} Ca^{2+}_{(aq)} + HCO^-_{3(aq)} \quad (4)$$

coupled with the following solution reactions

$$H^+_{(aq)} + HCO_{3(aq)} \rightleftharpoons H_2CO_{3(aq)} \rightleftharpoons CO_{2(aq)} + H_2O \quad (5)$$

leads to the loss of protons The detector electrode is thus effectively 'shielded'[13] from protons due to the dissolution process upstream The flux of protons, and hence current, at the electrode is reduced compared to the case where there is no heterogeneous reaction

Typical data for the flow rate dependence of the transport-limited current are shown in Figure 6 A finite dissolution process is indicated by the fact that the measured currents are less than those predicted theoretically for no heterogeneous reaction, but are larger than predicted for a transport-controlled (maximum reactivity) dissolution process A series of experiments carried out at several pH values pointed to a dissolution process (defined in terms of the interfacial flux of Ca^{2+}) governed by first order kinetics in the *interfacial* proton concentration, $[H^+]_s$ [13]

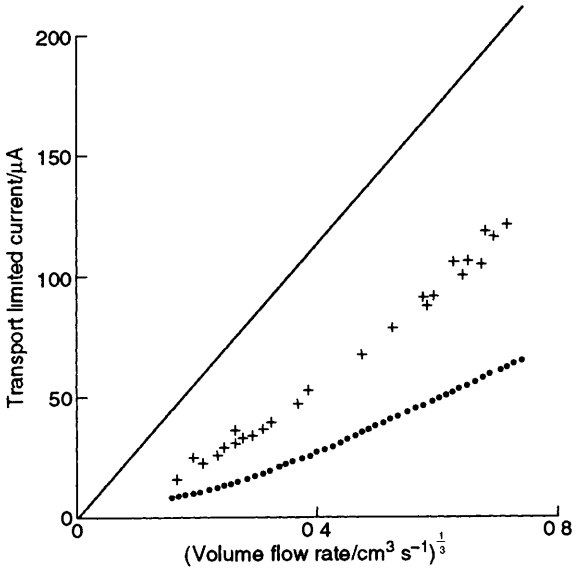

Figure 6 Flow rate dependence of the transport-limited current for the reduction of H^+ at a platinum detector electrode (+) after passage of the solution over a calcite crystal with the (100) face exposed The solid line shows the behaviour for the case where there is no reaction of H^+ at the crystal surface, while the dotted line shows the behaviour predicted theoretically for the transport-controlled reaction of H^+ with the crystal surface For this experiment, the bulk concentration of H^+ was 10^{-3} mol dm^{-3}, the crystal length was 0 180 cm, the detector electrode length was 0 055 cm, and $h = 0$ 013 cm
(Redrawn with permission from R G Compton and P R Unwin, *Philos Trans R Soc London Ser A*, 1990, **330**, 1)

$$j_{Ca} \text{ (mol cm}^{-2}\text{ s}^{-1}) = k'[H^+]_s \quad (6)$$

where k' was found to have the value 0 04 cm s^{-1}

As with the RDM, the CFMED treats the dissolving crystal surface as uniformly reactive, *i e* the derived value of k' is assumed to apply to the entire surface Some microscopic information is available through post-reaction investigations of the microtopography of the crystal surface [13 15] For example, in the case of the calcite (100) face, light microscopy revealed that dissolution at low pH proceeded through the formation of etch pits at sites on the surface where dislocations emerged [13(b)] Rhombohedral etch pits reflecting the morphology of the (100) cleavage plane were found to cover the surface, suggesting that the description of the dissolution process in terms of a single rate constant was realistic

For other dissolution systems,[14 15] the etch-pit morphologies revealed by post-reaction microscopy suggest that dissolution can be highly anisotropic even on a micrometer scale However, macroscopic techniques such as the CFMED and RDM are only able to measure the effective (average) dissolution rate of a surface In this situation, direct *in situ* microscopic probes of dissolution processes are proving to be extremely valuable, as described below

3.3 Flow Method with *In Situ* Interferometry and Microscopy

One approach to probing dissolution rates *in situ* at the microscopic level has been the recent development of an apparatus in which the concentration gradient at a single crystal/solution interface is determined directly *via* Mach–Zehnder interferometry, as an undersaturated solution is flowed over the surface of the crystal [23—25] In this interferometric technique, the arrangement of mirrors is such that the probe light beam is transmitted through the object unidirectionally, and as a consequence large changes in refractive index (resulting from concentration gradients) can be determined without complications from fringe broadening which may result from alternative interferometric techniques Phase contrast microscopy, differential interference contrast microscopy, or Michelson interferometry is employed in parallel to visualize in real time the dissolution[23 24] (or growth[26 27]) of a particular feature on the crystal surface

The technique has recently been used to monitor the formation and expansion of an individual etch pit, nucleated at a dislocation characterized by a ⟨110⟩ Burgers vector, emerging on the (111) face of potassium aluminium sulfate [24] The local dissolution characteristics were determined in real time by measuring the dissolution rate normal to the crystal, R, the average velocity of step retreat from the source of the etch pit in its lateral expansion, V, and the pit slope, P, as a function of the interfacial undersaturation As found in *ex situ* RDM studies,[12] pits were only nucleated at dislocation sites when the undersaturation in bulk solution

$$\sigma_b = 1 - S_b \quad (7)$$

exceeded a critical value of 0 026 In equation 7, S_b is the bulk saturation ratio, which, for a general ionic crystal, $M_\nu X_\nu$, is defined as

$$S_b = \left[\frac{(a_{M\ b})^\nu (a_{X^{\nu-}\ b})}{K_s} \right]^{1/\lambda} \quad (8)$$

where K_S is the solubility product of the solid material, λ is the number of ions in the formula unit of the ionic crystal, and $a_{i\,b}$ denotes the activity of species i (M^{z+} or $X^{\nu-}$) in bulk solution

Below the critical value of the bulk solution undersaturation, the surface undersaturation, σ_s, was found to be in close agreement with σ_b since, under these conditions, the crystal surface was effectively inert to dissolution However, once the critical bulk undersaturation was exceeded, dissolution of material from the crystal surface resulted in $\sigma_s < \sigma_b$, as shown in Figure 7 The results shown in this figure provide a convincing

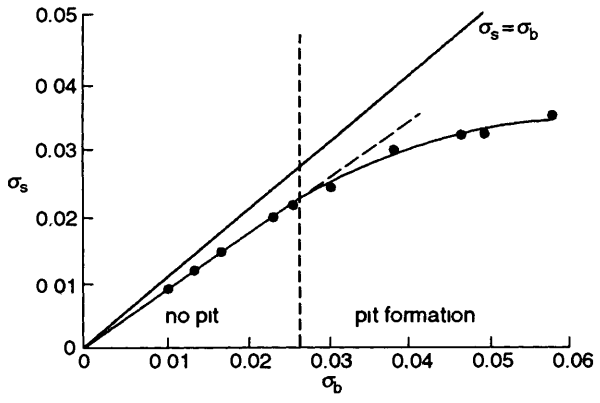

Figure 7 Relationship between the bulk undersaturation, σ_b, and surface undersaturation, σ_s, as an aqueous solution flows over the (111) face of a potassium aluminium sulfate single crystal, with a mean flow velocity of 10 cm s^{-1} The vertical dashed line denotes the bulk undersaturation threshold above which the formation of etch pits on dislocations with a ⟨110⟩ Burgers vector takes place
(Redrawn with permission from K Onuma, K Tsukamoto, and I Sunagawa, *J Cryst Growth*, 1991, **110**, 724)

demonstration that in the interpretation of crystal dissolution kinetics, σ_s should not always be assumed to be equal, or indeed linearly related, to σ_b

A major question in crystal dissolution and growth is whether the two processes are symmetrically related at the same point on a surface This problem was recently addressed for dislocations emerging on the (111) face of potassium aluminium sulfate, with a ⟨110⟩ Burgers vector [24] Over a range of interfacial undersaturations (and corresponding supersaturations), it was found that the step velocities, V, were essentially equal during dissolution and growth, but that the rate of dissolution normal to the surface, R, was considerably higher than the corresponding growth rate, as shown in Figure 8 This result confirmed earlier theoretical predictions of several groups [28] In essence, removal of material from the zone of the stress field around the apex of an emerging dislocation releases strain energy, and thereby provides an additional driving force for dissolution, which is not available for crystal growth

The flow method with *in situ* interferometry and microscopy goes a long way to directly addressing, at the microscopic level, questions (i) to (iii) posed at the start of this review It should be

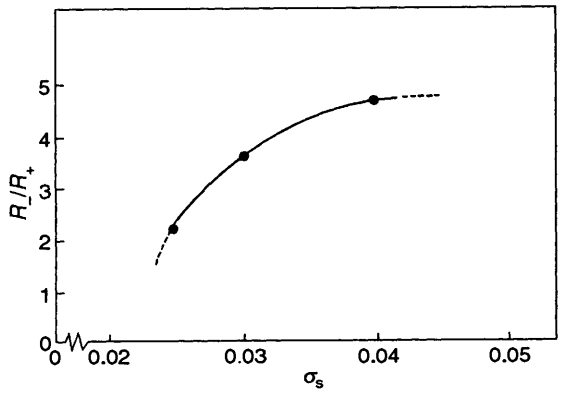

Figure 8 Ratio of the dissolution and growth rates normal to the crystal, R_-/R_+, at dislocation sites on the (111) face of potassium aluminium sulfate, characterized by a ⟨110⟩ Burgers vector, as a function of interfacial undersaturation for dissolution (and the equivalent supersaturation for growth) Data were obtained using the flow method with *in situ* interferometry and microscopy at a mean flow rate of 10 cm s^{-1}
(Redrawn with permission from K Onuma, K Tsukamoto, and I Sunagawa, *J Cryst Growth*, 1991, **110**, 724)

recognized, however, that the surface undersaturation measured by Mach–Zehnder interferometry represents an average value across the crystal in the direction of the optical light path In practice, a heterogeneously reactive surface would lead to a non-uniform interfacial undersaturation, and therefore introduce some error in the estimation of the undersaturation at the part of the interface of interest

4 Scanned Probe Microscopy Techniques

The development of scanned probe microscopy (SPM) methods has yielded a wealth of new information on the structure, reactivity, and many other properties of surfaces and interfaces at high spatial resolution [29] In the dissolution field, two SPM techniques, scanning electrochemical microscopy[30] and atomic force microscopy,[31] appear to be particularly promising as direct *in situ* probes of microscopic kinetics at the micrometer to nanometer level In this section we provide a brief introduction to these techniques and the type of information they can provide on the elementary mechanisms controlling crystal dissolution processes

4.1 Scanning Electrochemical Microscopy (SECM)

4 1 1 Principles

SECM employs an amperometric or potentiometric ultramicroelectrode (UME) – an electrode with a characteristic dimension, r, in the micrometer or submicrometer range – which is positioned or scanned in close proximity to a target interface (at a distance $d<r$) with the aid of piezoelectric positioning elements [30] The response of the electrode (or tip) can be used to provide local information on interfacial reactivity or topography, depending upon the nature of the experiment carried out [30]

The SECM arrangement for the study of ionic crystal dissolution kinetics is shown schematically in Figure 9(*a*) In this application, the tip UME is an amperometric (disc) working electrode in a standard two (or three) electrode arrangement, comprising a reference (and an auxiliary) electrode The UME is employed to induce and monitor dissolution, from a specific region of the crystal surface [32] This is achieved by stepping the electrode potential from a value at which no electrochemical reactions occur, and the solution is saturated with respect to the solid crystal, to a value at which the electrolysis of one (or more) types of the lattice ions in the solution occurs at a diffusion-controlled rate The resulting electrode process depletes the solution concentration of lattice ions in the gap between the tip and the crystal surface, and the undersaturation at the crystal/solution interface, located under the tip, provides the thermodynamic force for the dissolution reaction Dissolving ions diffuse from the crystal across the gap and are detected at the tip UME thus producing a current flow, the magnitude of which depends on the rate and mechanism of the dissolution reaction

The SECM approach allows questions (i) to (iii) outlined earlier to be addressed at the microscopic level First, mass transfer in the gap between the tip and the crystal surface occurs by diffusion alone, which is well defined [30] This allows the effects on the dissolution process of local mass transfer and interfacial undersaturation to be quantitatively characterized The concentration distribution of the species of interest can be calculated by solving the diffusion equation

$$\frac{\partial c}{\partial t} = D\left(\frac{1}{r}\frac{\partial c}{\partial r} + \frac{\partial^2 c}{\partial r^2} + \frac{\partial^2 c}{\partial z^2}\right) \qquad (9)$$

which is appropriate to the axisymmetric cylindrical SECM geometry,[30] subject to boundary conditions which define the chemical processes occurring at the tip and the crystal surface (*i e*, in the latter case, the dissolution reaction) In equation 9, t is time and c denotes concentration The remaining terms have either been defined earlier or can be understood by referring to Figure 9(*b*) The effective diffusion rate can be varied over a wide

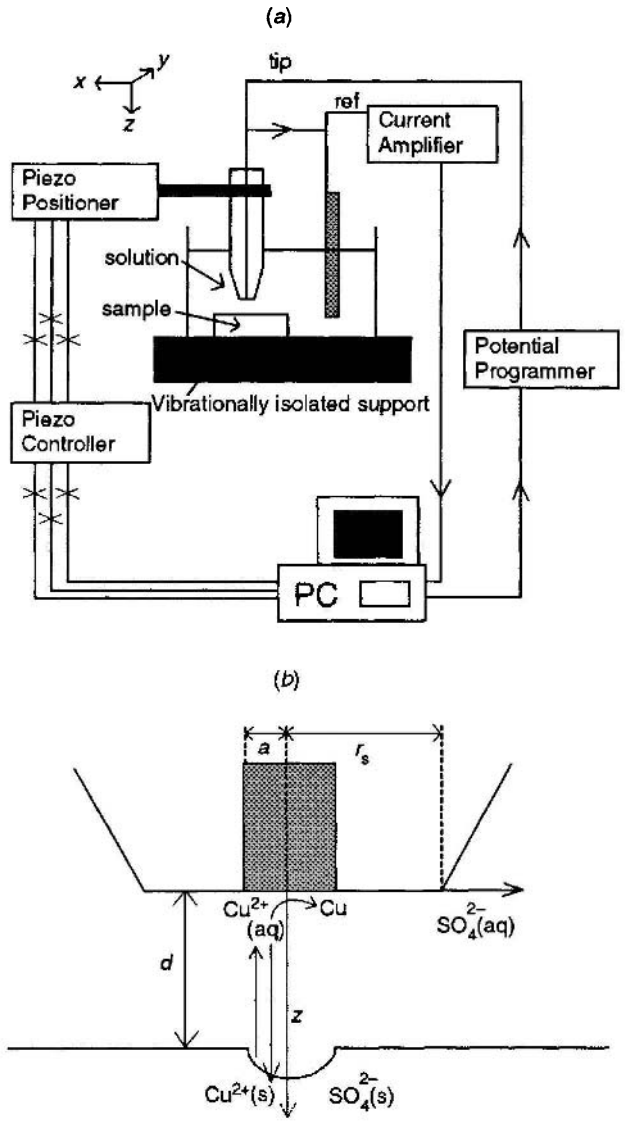

Figure 9 Schematics (not to scale) showing the instrumentation for, and principles of, SECM induced dissolution Figure (*a*) shows the instrument while (*b*) shows the processes occurring in the tip/crystal domain following induced dissolution, using copper sulfate pentahydrate as an example, where the solution is made undersaturated through the reduction of Cu^{2+} to Cu The latter diagram also shows the coordinate system used to describe the SECM geometry Note that typically $d < a \approx 0\,1\ r_S$

dynamic range by changing both the size of the UME and the tip/crystal separation [30] In particular, the close (sub-micrometer) tip/crystal separations which are attainable promote high rates of mass transfer, thereby facilitating the study of fast reactions [30]

Secondly, the dissolution process is induced at a specific microscopic area on the crystal surface directly under the tip The size of this zone is a function of the UME diameter, tip/crystal separation, and the interfacial kinetics, but for fast processes at close tip/crystal separations the spatial resolution of SECM approaches the dimensions of the UME [32] SECM thus opens up the possibility of directly monitoring the reactivity of a targeted micrometer-sized spot on a surface

Additional advantages arise from the use of UME chronoamperometry For example, the extent of dissolution can readily be controlled by varying the length of the potential step This is a key feature of SECM which has opened up the possibility of studying the dissolution kinetics of very soluble materials for the first time, through the ability to induce dissolution for short periods (down to several milliseconds) [33] It is now well established that UME voltammetry can also be conducted with a wide range of supporting electrolyte concentrations,[34] thereby allowing the role of 'inert' electrolytes and, indirectly, the nature of any surface charge effects, in dissolution processes to be characterized

4 1 2 Applications

SECM has been used to characterize the dissolution kinetics of two very soluble crystalline ionic materials in aqueous solutions copper sulfate pentahydrate[32 35 36] and potassium ferrocyanide trihydrate [33] Dissolution from the (100) face of triclinic copper sulfate pentahydrate single crystals grown from aqueous solution was initiated through the chronoamperometric reduction of Cu^{2+} to Cu at a platinum disc ultramicroelectrode (with a radius of 12 5 μm), placed at a series of distances normal to the crystal surface Experiments were carried out with solutions containing a range of sulfuric acid concentrations, which were saturated with respect to copper sulfate Sulfuric acid served as both a supporting electrolyte (to suppress migration effects) and a buffer of the sulfate ion concentration during an SECM measurement, thereby reducing the SECM mass transport problem to the consideration of a single-species as embodied in equation 8 Finally, under the defined conditions, dissolution occurred in a solution which was non-stoichiometric with respect to the concentrations of the lattice ions This provided the opportunity to test fundamental dissolution theories under conditions where experiments with particulate materials have suggested that classical theories, such as the Burton, Cabrera, and Frank (BCF) model,[37] break down [2a] The BCF model was originally developed for crystal growth from the vapour phase at steps arising from screw dislocations, but is often used to describe crystal dissolution in liquids In this context, the two limiting steps in dissolution are direct detachment from steps or surface diffusion (following detachment)

SECM revealed two types of behaviour in the dissolution of the (100) face In the centre of the face, where the average dislocation spacing was considerably less than the size of the UME probe, dissolution was found to occur at a steady rate Analysis of a large body of data in terms of both a first and a second-order process in the interfacial undersaturation indicated that the dissolution flux of Cu^{2+} from this region of the crystal surface was described by the following rate law

$$J_{Cu^{2+}}\ (\text{mol cm}^{-2}\ \text{s}^{-1}) = (2\,0 \times 10^{-6})\sigma_s \qquad (10)$$

This law arises as one of the limits to the BCF model,[37 2(e)] indicating that for this system the BCF model may be valid Mechanistically, this would suggest that dissolution occurs by the direct detachment of ions, with surface diffusion processes playing a negligible role

At the edges of the (100) face the apparent dislocation density, of 3×10^3—10^4 cm^{-2}, indicated that with the high spatial resolution of the SECM tip, there would be a large probability of the probe inducing dissolution in an area of the surface effectively devoid of dislocations In combination with the studies above, this provided the opportunity to assess the role of dislocations in the rate and mechanism of dissolution processes

A typical example of the chronoamperometric reponse observed when dissolution is initiated in a region close to the edges of this face is shown in Figure 10 The behaviour demonstrates that, in the absence of dislocations on the surface, SECM-induced dissolution occurs *via* a unique oscillatory mechanism Following an initial brief period of *ca* 300 ms in which the crystal is highly active to dissolution, the rate, as reflected in the UME current, rapidly decreases and thereafter dissolution occurs in a series of periodic 'bursts'

The dissolution sites responsible for the initially active surface were postulated to be associated with growth steps,[36] which are abundant on the surfaces of crystals grown from solution As

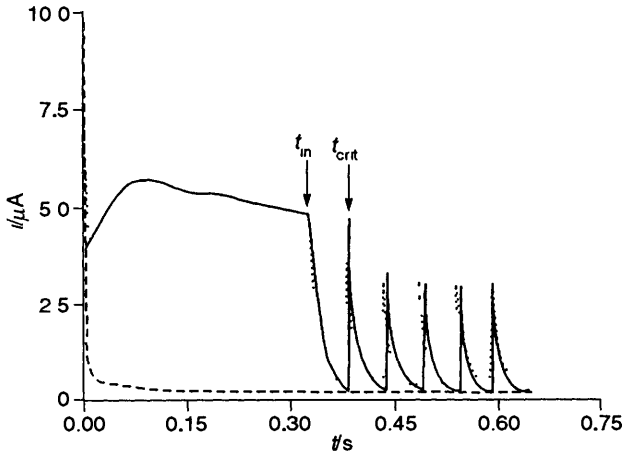

Figure 10 Experimental current – time characteristics for the reduction of Cu^{2+} at a platinum tip (a = 12 5 μm) positioned at a distance, d, of 1 0 μm from the copper sulfate pentahydrate (100) face, in an area of the crystal with a low dislocation density (—) The aqueous solution contained 3 6 mol dm $^{-3}$ H_2SO_4 and was initially saturated with respect to copper sulfate pentahydrate Also shown is the best fit of the data to an SECM oscillatory dissolution model ( )[38] using the parameters cited in the text, along with the behaviour predicted for an inert surface (---) [30]

dissolution proceeds, these steps retreat out of the SECM zone, and, in the absence of dislocations in the area probed by the UME, the targeted part of the surface becomes depleted of active sites This process results in a decrease in the dissolution rate, which is reflected in a drop in the current flowing at the tip, at the time marked t_{in} in Figure 10 It has been shown that dissolution in this initial period (0–t_{crit}) can be successfully modelled in terms of the following rate law, describing the flux of Cu^{2+}, from the crystal surface [36 38]

$$D\frac{\partial c}{\partial z} = -k_d\sigma_s\theta \tag{11}$$

coupled with the following conditions on the fraction of active dissolution sites

$$0 < t \leq t_{in} \qquad \theta = 1 \tag{12}$$

$$t_{in} < t \leq t_{crit} \qquad \frac{\partial\theta}{\partial t} = -\frac{k_d\sigma_s\theta}{N} \tag{13}$$

In equations 11 to 13 k_d is the dissolution rate constant, which was found to have the value of 3 9 × 10^{-6} mol cm^{-2} s^{-1}, and N is the density of surface Cu^{2+} removed during each burst in dissolution activity (related to the number of layers of copper sulfate removed)

The decrease in crystal activity, at t_{in}, coupled with strongly hindered radial diffusion in the SECM configuration,[30] results in a corresponding rapid depletion in the concentration of electroactive material in the tip/crystal gap and, in particular, at the crystal/solution interface [36 38] Eventually, the undersaturation at the crystal/solution interface attains a sufficiently high value for the spontaneous nucleation of fresh dissolution sites, and dissolution is reinitiated at the corresponding time, t_{crit} [36 38] The rate (*i e*, current) rapidly peaks, and then decreases as active sites are lost from the surface The process outlined above is repeated, producing the current oscillations Numerical modelling of mass transport in the SECM domain[38] allowed the critical interfacial saturation ratio, necessary to initiate dissolution in the absence of dislocations, to be identified as 4 5 × 10^{-4}, while *ca* 100 monolayers of the crystal were found to be stripped away during each surge in dissolution activity The results obtained have been interpreted elsewhere in terms of classical nucleation theories for dissolution [36 38]

Studies of dissolution from the (010) face of monoclinic potassium ferrocyanide trihydrate, in solutions containing 3 5 mol dm^{-3} potassium chloride, were recently carried out to examine whether classical models applied to the dissolution of an unsymmetric salt in non-stoichiometric solutions of the lattice ions [33] The reaction was investigated using SECM chronoamperometry at platinum disc UMEs, by stepping the potential of the tip, positioned close to the crystal surface, to a value at which the oxidation of ferrocyanide to ferricyanide occurred at a diffusion-controlled rate By making measurements with a series of increasingly small tip sizes (UMEs with radii of 12 5 μm down to 2 5 μm) and tip/crystal separations, the reaction was pushed from a position where the initial rate was effectively diffusion controlled, to a timescale where surface kinetic limitations were apparent Interpretation of initial rate data in terms of suitable candidate rate laws suggested that the rate was governed by a second order term in the interfacial undersaturation at the crystal/solution interface This was shown to be consistent with the BCF model at low interfacial undersaturations,[37] and pointed to surface diffusion as the rate limiting step in the dissolution process

The potassium ferrocyanide trihydrate system was shown to be a useful first model for testing the abilities of the SECM to image the dissolution activity over a single crystal surface [33] In these dissolution rate imaging experiments the current for the oxidation of ferrocyanide was recorded as a function of tip position, as the UME was scanned at a constant height over the crystal surface Additionally, by adding a small concentration of ferricyanide to the solution, the reduction of which served as a calibrant of the tip/crystal distance,[30] it was demonstrated that the topography and dissolution activity of a single crystal surface could be mapped in sequential scans at the micrometer level Typical results of this type are summarized in Figure 11 For this particular experiment, the ability of the SECM to image topography was tested by creating a surface feature in which a pit was electrochemically pre-etched in the surface of the crystal, and the crystal surface was then deliberately misoriented by *ca* 1° to the plane in which the tip was scanned

4.2 Atomic Force Microscopy (AFM)

4 2 1 Basic Principles

AFM[31] maps the topography of a sample through a sharp tip, typically composed of Si_3N_4, attached to the end of a cantilever The tip is held in close proximity to the surface of a sample (attached to an *xyz* piezoelectric positioner), which is scanned underneath the tip, in a raster pattern, in the *xy* plane Deflections in the cantilever, due to attractive or repulsive forces (depending on the mode of operation), are usually detected by a laser beam reflected from the back of the cantilever into a position-sensing diode (although several other detection procedures are available[39]) In the constant force imaging mode, a feedback loop is used to keep the force between the tip and sample constant, and the z element of the piezoelectric positioner adjusts to maintain the reflected beam position constant Relative displacements of the z axis then trace changes in the height of the surface, which are measured as a function of the relative tip/sample position in the *xy* plane

The advent of AFM[40] has opened up the possibility of studying topographical changes on dissolving surfaces, in real time, with nanometer resolution In particular, AFM has the potential to assess directly the validity of classical dissolution theories, such as the BCF model,[37] at the atomic level, by imaging the retreat of monatomic steps during the dissolution of a surface Initial work in this area focused on *ex situ* imaging of crystal surfaces in air after they had been subjected to dissolution,[41] but the development of several types of AFM fluid cells,[42 44] some with dynamic flow capabilities[43 44] such as that shown in Figure 12, has recently led to *in situ* studies of dissolution processes,[43 45 47] under conditions where the rate of fluid flow over the crystal surface can be controlled The

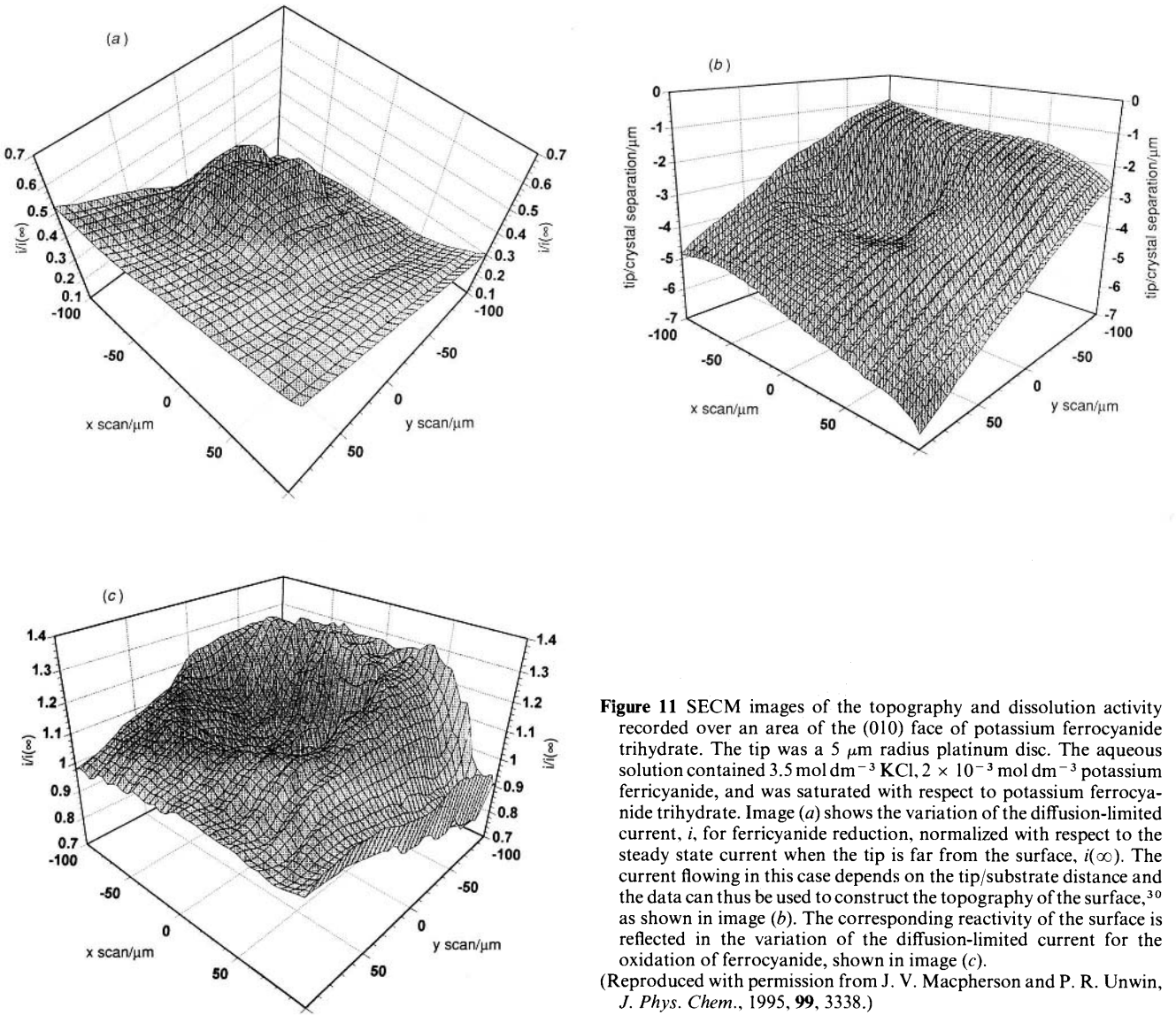

Figure 11 SECM images of the topography and dissolution activity recorded over an area of the (010) face of potassium ferrocyanide trihydrate. The tip was a 5 μm radius platinum disc. The aqueous solution contained 3.5 mol dm^{-3} KCl, 2 × 10^{-3} mol dm^{-3} potassium ferricyanide, and was saturated with respect to potassium ferrocyanide trihydrate. Image (*a*) shows the variation of the diffusion-limited current, *i*, for ferricyanide reduction, normalized with respect to the steady state current when the tip is far from the surface, $i(\infty)$. The current flowing in this case depends on the tip/substrate distance and the data can thus be used to construct the topography of the surface,[30] as shown in image (*b*). The corresponding reactivity of the surface is reflected in the variation of the diffusion-limited current for the oxidation of ferrocyanide, shown in image (*c*).
(Reproduced with permission from J. V. Macpherson and P. R. Unwin, *J. Phys. Chem.*, 1995, **99**, 3338.)

relatively slow time resolution of AFM (tens of seconds per image) has so far limited the technique to systems with slow dissolution rates, but, nevertheless, fundamental information has been obtained on a range of systems, including the dissolution of the calcite cleavage plane in aqueous solutions,[43,45] the L-leucine (100) surface in propanol,[46] the lithium fluoride (100) surface,[44] the L-ascorbic acid (100) face,[44] and the (010) face of gypsum in aqueous solution.[47] Although fluid flow past the AFM tip can affect the quality of AFM images, a recent study has demonstrated that atomic level resolution is possible with moderate flow rates.[48]

4.2.2 Nanometer-level Features Detected by AFM

As outlined earlier in this review, the nucleation and expansion of etch pits is an important mechanism in the dissolution of crystals. The high resolution achievable with AFM has allowed the initial stages of this process to be monitored on a scale previously unattainable.[41,43,45,47] In an *ex situ* study of quartz surfaces, following dissolution at 148 °C and 211 °C in 0.01 mol dm^{-3} aqueous KOH, AFM identified shallow-walled pits on reacted surfaces which were undetectable by optical microscopy and high resolution electron microscopy.[41] A typical etch pit is shown in Figure 13. This consists of a central flat base with an area of 50 nm by 100 nm, bordered by shallow walls, which comprise a series of widely spaced ledges, either one or two

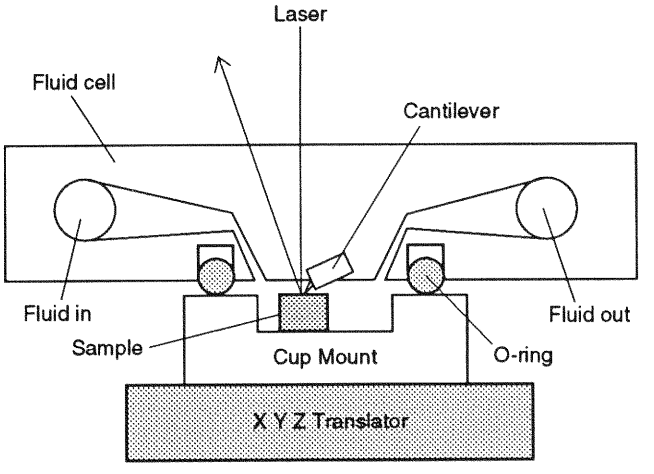

Figure 12 Schematic of an AFM fluid flow cell showing the entry and exit ports for the fluid, the cantilever tip in contact with a sample surface, and a positioning sensing laser beam reflecting from the back of the cantilever.
(Redrawn with permission from P. E. Hillner, A. J. Gratz, S. Manne, and P. K. Hansma, *Geology*, 1992, **20**, 359.)

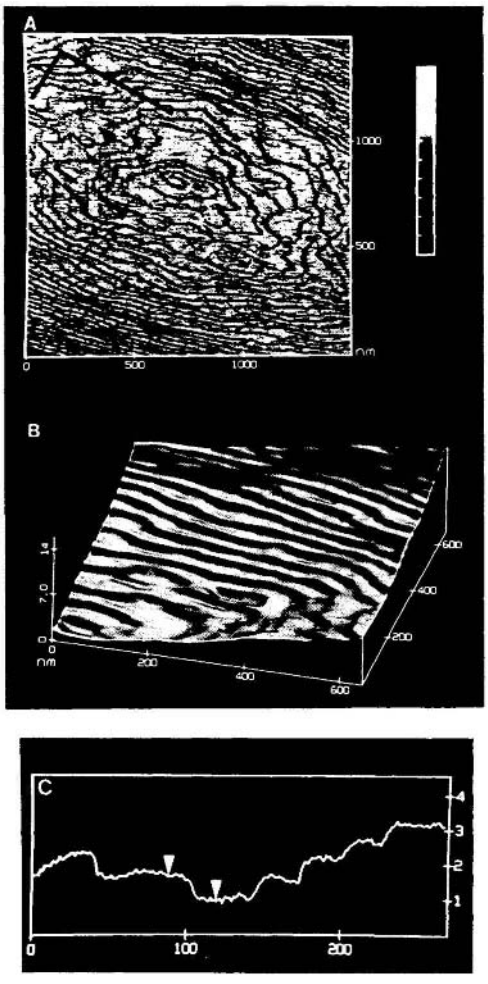

Figure 13 AFM images of an etch pit on quartz, formed through dissolution at 148 °C in 0.01 mol dm^{-3} aqueous KOH, and then imaged in ethanol with an applied force $\leq 10^{-8}$ N. (A) Image shown in the illumination mode. The height difference between the bottom of the pit and the highest point on the image is *ca.* 20 nm. The bars indicate the ⟨c⟩ and ⟨a⟩ directions. (B) A surface plot of one quadrant of the pit. (C) Profile across the pit floor in the ⟨a⟩ direction. This figure shows wide terraces (*ca.* 30 nm long) separated by distinct steps. The height between the cursors is 0.7 nm.
(Reproduced with permission from A. J. Gratz, S. Manne, and P. K. Hansma, *Science*, 1991, **251**, 1343.)

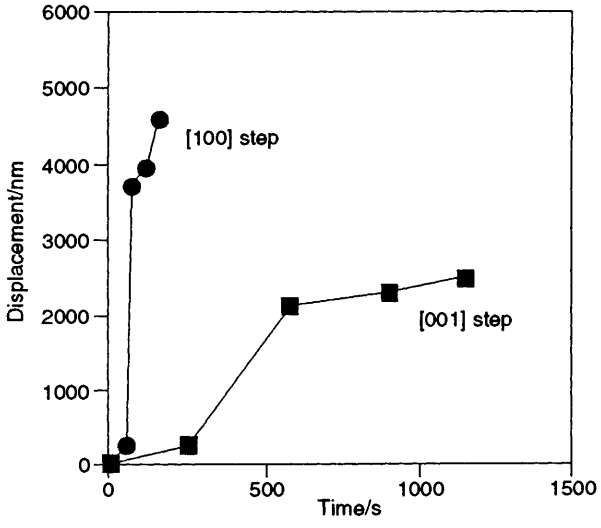

Figure 14 Displacement of monolayer steps with time for two isolated steps, with different orientations, on the (010) surface of gypsum during dissolution in an aqueous flowing undersaturated solution ($S_b = 0.65$).
(Redrawn with poermission from D. Bosbach and W. Rammensee, *Geochim. Cosmochim. Acta*, 1994, **58**, 843.)

monolayers in height. This result provided direct molecular-level support for dissolution models based on ledge motion.[37] The shallowness of the pits observed in quartz dissolution indicates that radial dissolution dominates over core dissolution, while the ellipticity indicates that dissolution is strongly surface-direction dependent.[41]

More recently, AFM was used to measure the spatial distribution and expansion of pits nucleated on the (010) surface of gypsum, in contact with an undersaturated flowing solution.[47] Pits bordered by steps running parallel to the [100] and [001] directions were found to be elongated in the latter direction, demonstrating that dissolution was anisotropic, occurring faster in the [100] direction. This study[47] also reported quantitative measurements of the velocities of isolated monolayer steps of different orientations, by monitoring step displacement as a function of time in several successive scans over the same area of the crystal surface. Typical results for a [100] step and [001] step are shown in Figure 14.[47] With flow rates in the range 16—50 μL s^{-1}, and a bulk saturation ratio, S_b, of 0.65, [100] steps moved at 30 nm s^{-1}, [101] steps at 9.5 nm s^{-1} and [001] steps at 2.5 nm s^{-1}. Surface microtopography was shown to have a strong influence on the rates at which these steps moved. In areas where the step density was high, all steps were found to move at slower rates than the isolated step.[47] This was attributed to mass transport limiting the rate at all of the flow rates employed.[48] In addition to monitoring step dynamics in undersaturated solutions, experiments carried out with saturated solutions demonstrated the existence of kink sites – the elementary reactive sites involved in the propagation of dissolving steps (see Figure 2) – along [001] steps on the surface. Moreover, kink densities of 0.16—0.27 measured by AFM were found to be in good agreement with the value of 0.21 predicted theoretically for this system by Monte Carlo simulation methods.[47]

Dissolution, through the recession of steps, has also been observed on the (100) face of L-leucine.[46] In general, steps oriented parallel to the ⟨010⟩ directions were all found to move at about the same speed, which was independent of the interstep spacing and inconsistent with the BCF model[37] for dissolution controlled by surface diffusion. Anisotropy in local dissolution rates was observed such that bends in the ⟨010⟩ steps, oriented in the ⟨001⟩ direction, were found to move at rates between one and ten times faster than ⟨010⟩ steps.[46] Moreover shorter bends were observed to move faster than longer bends. This was attributed to the larger mass flux at the latter creating a local partially saturated solution on top of the bend, which served to slow down the reaction kinetics.[46]

Although only a few dissolution studies with AFM have been reported, considerable insights into the nanometer-level structural changes accompanying dissolution processes have been obtained. The development of flow-through AFM techniques has been valuable in observing dissolution processes *in situ*, but the nature of mass transport in the vicinity of the tip has not yet been fully studied. In order for AFM to probe dissolution under conditions where local mass transport is well defined, further work is required on the design of AFM cells and the modelling of mass transport within them. As with all SPM methods, the range of dynamic surface phenomena accessible is governed by the image acquisition time, and the study of faster processes will require developments in instrumentation and imaging techniques.

5 Conclusions and Perspectives

The aim of this review has been to show the rapid progress that has taken place in the study of dissolution kinetics in recent

years Learning from the established surface science field, there has been a general move away from the ill-defined surfaces associated with powdered materials to the use of single crystals In several experimental techniques, such as the rotating disc method and channel flow method, this has been coupled with the employment of controlled mass transport This has allowed the competition between transport and surface kinetic effects to be investigated, and the role of interfacial undersaturations as the driving force for dissolution to be explored

Even on a single crystal surface, dissolution rates can be strongly space dependent Recent techniques such as the channel flow method with interferometry and microscopy detection and scanning electrochemical microscopy are proving to be valuable in resolving local reactivity problems which can be addressed at the micrometer level, under controlled mass transport conditions Moving to higher resolution, atomic force microscopy has proved to be extremely valuable in directly confirming the operation of a number of fundamental processes which underpin established dissolution theories

Studies with local techniques are still very much in the early stages Although recent progress has been rapid and significant, our understanding of crystal dissolution processes still lags behind that of other areas of solid/liquid interfacial chemistry, such as reactions at the electrode/electrolyte interface Moreover, studies of the solid/liquid interface, in general, have a long way to go to catch up with the body of knowledge on metals and semiconductor surfaces in ultra high vacuum However, if future developments continue at the pace seen in the last few years, a comprehensive understanding of the factors controlling crystal dissolution and growth at the molecular level appears to be achievable

Acknowledgments The support of our SECM dissolution programme by the EPSRC is gratefully acknowledged

6 References and Notes

1 A W Adamson, 'Physical Chemistry of Surfaces', John Wiley, New York, 5th Edn , 1990

2 For earlier reviews see for example (*a*) H G Linge, *Adv Colloid Interface Sci* , 1981, **14**, 239, (*b*) B Simon, in 'Interfacial Aspects of Phase Transformations', *NATO ASI Ser C*, ed B Mutaftschiev, D Reidel, The Netherlands, 1982, vol 87, p 639, (*c*) I G Gorichev and N A Kipriyanov, *Russ Chem Rev* , 1984, **53**, 1039, (*d*) K Sangwal, 'Etching of Crystals, Theory, Experiment and Application', North Holland, Amsterdam, 1987, (*e*) J W Zhang and G H Nancollas, *Rev Mineral* , 1990, **23**, 365

3 R B Heimann, in 'Crystals Growth, Properties and Applications', ed J Grabmaier, Springer-Verlag, Berlin, 1982, p 173

4 (*a*) A E Blum and A C Lasaga, in 'Aquatic Surface Chemistry', ed W Stumm, John Wiley, New York, 1987, p 255, (*b*) W Stumm and E Weiland, in 'Aquatic Chemical Kinetics', ed W Stumm, John Wiley, New York, 1990, p 367

5 See for example 'Biological Mineralization and Demineralization', ed G H Nancollas, Springer-Verlag, Berlin, 1982

6 T K Sherwood, R L Pigford, and C R Wilke, 'Mass Transfer', McGraw-Hill, New York, 1975

7 E L Sjoberg and D Rickard, *Geochim Cosmochim Acta*, 1983, **47**, 2281

8 For a review see A F M Barton and S R McConnel, *Chem Aust* , 1979, **46**, 427

9 (*a*) A F M Barton and S R McConnel, *Trans Faraday Soc* , 1971, **48**, 2847, (*b*) D R Boomer, C C McCune, and H S Fogler, *Rev Sci Instrum* , 1972, **43**, 225, (*c*) K Lund, H S Fogler, C C McCune, and J W Ault, *Chem Eng Sci* , 1973, **28**, 691, (*d*) G H Nancollas and H G Linge, *Calcif Tissue Res* , 1973, **12**, 193, (*e*) K Lund, H S Fogler, C C McCune, and J W Ault, *Chem Eng Sci* , 1975, **30**, 825, (*f*) V K Cheng, B A W Coller, and J L Powell, *Faraday Discuss Chem Soc* , 1984, **77**, 243, (*g*) R G Compton and P J Daly, *J Colloid Interface Sci* , 1984, **101**, 159, (*h*) D E Giles, I M Ritchie, and B -A Xu, *Hydrometallurgy*, 1993, **32**, 119

10 D T Rickard and E L Sjoberg, *Am J Sci* , 1983, **283**, 815

11 (*a*) V P Karshin and V A Grigoryan, *Russ J Phys Chem* , 1970, **44**, 762, (*b*) L A Virtsava, Yu R Dzelme, Yu E Tilkis, and L T Bugaenko, *Russ J Phys Chem* , 1978, **52** 1638, (*c*) E L Sjoberg and D T Rickard, *Geochim Cosmochim Acta*, 1984, **48**, 485, (*d*) E L Sjoberg and D T Rickard, *Chem Geol* , 1984, **42**, 119, (*e*) E L Sjoberg and D T Rickard, *Chem Geol* , 1985, **49**, 405, (*f*) R G Compton, P J Daly, and W A House, *J Colloid Interface Sci* , 1986, **113**, 12, (*g*) R G Compton and P J Daly, *J Colloid Interface Sci* , 1987, **115**, 493, (*h*) I N MacInnis and S L Brantley, *Geochim Cosmochim Acta*, 1992, **56**, 1113, (*i*) I N MacInnis and S L Brantley, *Chem Geol* , 1993, **105**, 31

12 B van der Hoek, W J P van Enckevort, and W H van der Linden, *J Cryst Growth*, 1983, **61**, 181

13 (*a*) R G Compton, K L Prichard, and P R Unwin, *J Chem Soc Chem Commun* , 1989, 249, (*b*) R G Compton and P R Unwin, *Philos Trans R Soc London Ser A*, 1990, **330**, 1

14 (*a*) R G Compton, K L Prichard, P R Unwin, G Grigg, P Silvester, M Lees, and W A House, *J Chem Soc Faraday Trans 1*, 1989, **85**, 4335, (*b*) A J Barwise, R G Compton, and P R Unwin, *J Chem Soc Faraday Trans* , 1990, **86**, 137, (*c*) R G Compton and P R Unwin, *J Chem Soc Faraday Trans* , 1990, **86**, 1517

15 R Orton and P R Unwin, *J Chem Soc Faraday Trans* , 1993, **89**, 3947

16 R G Compton, C T Walker, P R Unwin, and W A House, *J Chem Soc Faraday Trans* , 1990, **86**, 849

17 (*a*) R G Compton and K L Prichard, *Philos Trans R Soc London Ser A*, 1990, **330**, 47, (*b*) C A Brown, R G Compton, and C A Narramore, *J Colloid Interface Sci* , 1993, **160**, 372

18 R G Compton and C A Brown, *J Colloid Interface Sci* , 1994, **165**, 445

19 See for example A J Bard and L R Faulkner, 'Electrochemical Methods', John Wiley, New York, 1980, ch 8

20 V G Levich, 'Physicochemical Hydrodynamics', Prentice Hall, Englewood Cliffs, NJ, 1962

21 P R Unwin and R G Compton, in 'Comprehensive Chemical Kinetics', ed R G Compton and A Hamnett, Elsevier, Amsterdam, 1989, vol 29, p 173

22 P R Unwin, A J Barwise, and R G Compton, *J Colloid Interface Sci* , 1989, **128**, 208

23 I Sunagawa, *Aquat Sci* , 1993, **55**, 347

24 K Onuma, K Tsukamoto, and I Sunagawa, *J Cryst Growth*, 1991, **110**, 724

25 P G Vekilov, Yu G Kuznetzov, and A A Chernov, *J Cryst Growth*, 1990, **102**, 706

26 H Ohmoto, K Hayashi, K Onuma, K Tsukamoto, A Kitakaze, Y Nakano, and Y Yamamoto, *Nature (London)*, 1991, **351**, 634

27 K Maiwa, K Tsukamoto, and I Sunagawa, *J Cryst Growth*, 1990, **102**, 43

28 (*a*) N Cabrera and M M Levine, *Phil Mag* , 1956, **1**, 459, (*b*) B van der Hoek, J P van der Eerden, and P Benema, *J Cryst Growth*, 1982, **56**, 621, (*c*) B van der Hoek, J P van der Eerden, P Bennema, and I Sunagawa, *J Cryst Growth*, 1982, **58**, 365

29 For reviews, see for example 'Scanning Tunneling Microscopy and Related Techniques', ed R J Behm, N Garcia, and H Rohrer, *NATO ASI Ser E*, Kluwer, The Netherlands, 1990, vol 184

30 For general reviews, see for example (*a*) A J Bard, F -R F Fan, M V Mirkin, in 'Electroanalytical Chemistry', ed A J Bard, Marcel Dekker, New York, 1993, vol 18, p 243, (*b*) A J Bard, P R Unwin, D O Wipf, and F Zhou, *Am Inst Phys Conf Proc* , 1992, **254**, 235, (*c*) A J Bard, F -R F Fan, D T Pierce, P R Unwin, D O Wipf, and F Zhou, *Science*, 1991, **254**, 68

31 For a general introductory review, see for example D Rugar and P K Hansma, *Physics Today*, October 1990, p 23

32 J V Macpherson and P R Unwin, *J Phys Chem* , 1994, **98**, 1704

33 J V Macpherson and P R Unwin, *J Phys Chem* , 1995, **99**, 3338

34 See for example K B Oldham, in 'Microelectrodes Theory and Applications', *NATO ASI Ser E*, Kluwer, The Netherlands, 1991, vol 197, p 83

35 J V Macpherson and P R Unwin, *J Chem Soc Faraday Trans* , 1993, **89**, 1883

36 J V Macpherson and P R Unwin, *J Phys Chem* , 1994, **98**, 11764

37 W K Burton, N Cabrera, and F C Frank, *Philos Trans R Soc London Ser A*, 1951, **243**, 299

38 The theory in ref 36 has been further developed in J V Macpherson and P R Unwin, in preparation

39 C F Quate, *Surf Sci* , 1994, **299/300**, 980

40 G Binnig, C F Quate, and Ch Gerber, *Phys Rev Lett* , 1986, **56**, 930

41 A J Gratz, S Manne, and P K Hansma, *Science*, 1991, **251**, 1343

42 P A Johnson, C M Eggleston, and M F Hochella, *Am Mineral* , 1991, **76**, 1442

43 P E Hillner, A J Gratz, S Manne, and P K Hansma, *Geology*, 1992, **20**, 359

44 S Kıpp, R Lacmann, and M A Schneeweıss, *J Cryst Growth*, 1994, **141**, 291
45 P E Hıllner, S Manne, A J Gratz, and P K Hansma, *Ultramıcroscopy*, 1992, **42—42**, 1387
46 S Manne, J P Cleveland, G D Stucky, and P K Hansma, *J Cryst Growth*, 1993, **130**, 333
47 D Bosbach and W Rammensee, *Geochım Cosmochım Acta*, 1994, **58**, 843
48 W V Schmıdt and R C Alkıre, *J Electrochem Soc*, 1994, **141**, L85